



Improving local mean stress estimation using Bayesian hierarchical modelling

Yu Feng^a, Ke Gao^{b,*}, Arnaud Mignan^{a,b}, Jiawei Li^a

^a Institute of Risk Analysis, Prediction and Management (Risks-X), Academy for Advanced Interdisciplinary Studies, Southern University of Science and Technology, Shenzhen, China

^b Department of Earth and Space Sciences, Southern University of Science and Technology, Shenzhen, China

ARTICLE INFO

Keywords:

In situ stress
Bayesian hierarchical model
Uncertainty quantification
Information borrowing

ABSTRACT

Local mean stress state is an important parameter to many rock mechanics and geomechanics applications, yet its estimation may be subject to large uncertainty owing mainly to the usual limited number of high-quality stress data and the potentially significant natural variability of stresses in a rock volume. Hence, it is essential to quantify and reduce uncertainty in local mean stress estimation. This paper proposes a novel Bayesian hierarchical model that both probabilistically quantifies uncertainty in local mean stress estimation and allows logical borrowing of information across stress data from nearby locations. By application to both real-world and simulated stress data, our results show that the hierarchical model can improve local mean stress estimation simultaneously at each location in terms of uncertainty reduction in comparison to the customary approach. This improved probabilistic estimation has further benefits in that it not only allows for probabilistic implementation of further analyses in other applications involving mean stresses, but also gives more accurate analysis results.

1. Introduction

Knowledge of *in situ* stress state is of great importance for a wide range of rock mechanics and geomechanics applications, such as rock engineering design, hydraulic fracturing evaluation, nuclear waste deposition, groundwater flow analysis, mineral and petroleum extraction, and earthquake prediction.^{1–6} In these applications, local mean stress – an indicator of the overall stress state in a local rock volume – is often of interest as an input parameter, and is usually estimated using the average of a number of stress tensors measured from this location.^{7–14} This estimation practice can be written as:

$$\hat{S} = \frac{1}{n} \sum_{i=1}^n S_i = \frac{1}{n} \sum_{i=1}^n \begin{bmatrix} \sigma_{x_i} & \tau_{xy_i} & \tau_{xz_i} \\ & \sigma_{y_i} & \tau_{yz_i} \\ \text{sym.} & & \sigma_{z_i} \end{bmatrix}, \quad (1)$$

where $\hat{S} \in \mathbb{R}^{3 \times 3}$ is the estimate of the local mean stress tensor, $S_i \in \mathbb{R}^{3 \times 3}$ is the i th measured stress tensor, and σ and τ are the normal and shear tensor components with respect to a common x - y - z Cartesian coordinate system, respectively. Further, the eigenvalues and eigenvectors of \hat{S} are taken to be the estimates of the magnitudes and orientations of the principal mean stress state, respectively.

Statistically speaking, the estimate \hat{S} is only a point estimate of the unknown mean stress state in the local volume of interest given

measured stresses. However, such point estimation may be subject to large uncertainty owing mainly to the usual limited number of high-quality stress data and the potentially significant natural variability of stresses within a local rock volume.^{2,15–19} Also, potential measurement error and inadequacy of the statistical model may contribute to uncertainty in the resulting mean stress estimates. Hence, it is crucial to probabilistically quantify such uncertainty, as it allows for quantitative assessment of the reliability of estimated mean stresses and also facilitates application of more rational probabilistic analyses in, e.g., rock engineering design and earthquake risk assessment. For this reason, in a previous work, the authors proposed a Bayesian multivariate model that can probabilistically quantify uncertainty in mean stress estimation and demonstrated that the usual small numbers of stress data tend to yield unreliable mean stress estimates.²⁰

Following this, a question that is commonly asked by practitioners is how the local mean stress estimation may be improved by utilizing stress information from other sources. In practice, many additional sources could be available to provide at least partial information on the local mean stress state at no or low cost, and they include stress data measured from nearby locations, the commonly-assumed linear relation between vertical stress and burial depth, borehole breakouts, drilling-induced tensile fractures, fault-slip analysis, earthquake focal

* Corresponding author.

E-mail address: gaok@sustech.edu.cn (K. Gao).

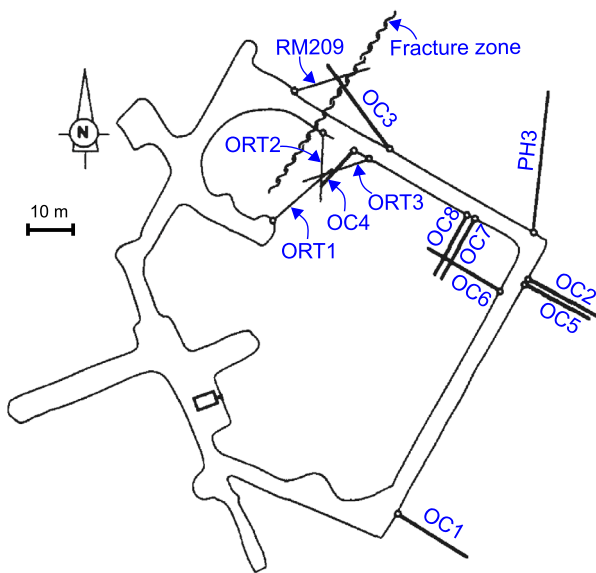


Fig. 1. Plan view of the 240 level of the AECL's URL showing the locations of 13 boreholes of overcoring stress measurements [after⁹].

mechanisms, core diskings, geological indicators and the like.^{2,3,21,22} Being able to use these additional stress information sources would be highly valuable, since the common stress measurement methods (e.g., hydraulic fracturing and overcoring) are both time-consuming and costly. Unfortunately, a logical framework to combine stress information from different sources is still lacking thus far. In several earlier works by the authors, we have demonstrated the potential of the Bayesian approach to formally incorporate additional stress information into stress estimation via informative prior distributions, but also highlighted some key challenges in eliciting appropriate informative priors from individual stress information sources.^{20,23}

Among the additional stress information sources, stress data from nearby locations may be a particularly important one, because they are generally available at the scale of interest and provide roughly the same level of data quality as the immediate stress data at hand. Especially in civil and mining engineering projects, stress measurements are often made in multiple boreholes on the same level or within a small domain. As an example, Fig. 1 shows the locations of 13 nearby boreholes on the 240 level (roughly a 60 m × 60 m domain) in the Underground Research Laboratory (URL) of the Atomic Energy of Canada Limited (AECL) in Manitoba, Canada, in which a total of 100 high-quality stress tensors were measured using the overcoring method.⁹ In such a case, the stress data from each borehole are customarily averaged independently to be taken as the estimate of the local mean stress state at the location of that borehole. However, based on our general understanding of stresses in rocks, stress states at nearby locations may have some degree of similarity rather than being either entirely different or identical, and thus may inform each other to a certain extent.

In the Bayesian framework, while informative priors provide a means of incorporating information from other sources, they are not sufficient for local mean stress estimation in the context of multiple stress data groups from nearby locations. The main reasons are twofold. First, each individual stress group rather than only one group may borrow, more or less, some information from the other groups, but using informative priors does not allow such adaptive borrowing of information simultaneously for local mean stress estimation for each individual group. Second, constructing informative priors from stress data at nearby locations is a manual task involving some subjectivity. For data structured in groups (e.g., stress data from nearby locations

herein and data compiled from multiple studies), a more objective and flexible approach to borrowing of information across groups is to implement hierarchical models (also known as multilevel models), which are known for their ability of accommodating possible similarity between data groups.^{24,25} Hierarchical models are extensively used as a method for combining information from multiple similar studies (known as meta-analysis) in the fields of medical research, social science, ecology and public health,^{24–31} and have recently gained attention in geotechnical and geophysical data analysis.^{32–38}

In this paper, we present a novel Bayesian hierarchical model for analysis of multiple stress data groups from nearby locations and demonstrate how the proposed hierarchical model can give improved local mean stress estimation simultaneously at each individual location compared to the customary approach in terms of uncertainty reduction. To this end, the remainder of this paper is organized as follows. Section 2 first concisely introduce the basics of hierarchical modelling along with two alternative conventional modelling approaches (i.e., no pooling and complete pooling) when dealing with data which are structured in groups, and then give the formulations of the three models for local mean stress estimation in the context of multiple stress data groups measured from nearby locations. Section 3 presents application of the three models to real-world stress data groups to demonstrate how the Bayesian hierarchical model improves mean stress estimation for each location, followed by a simulation study to further demonstrate the efficacy of the hierarchical model using simulated stress data in Section 4. Section 5 presents a discussion of the results, before a summary and conclusions provided in Section 6.

This paper explicitly focuses on novel application of Bayesian hierarchical modelling to improved statistical estimation of the mean stress state at a location by means of borrowing information from stress tensor data measured from nearby locations. Hence, a detailed account of stress measurement methods regarding their theory, equipment and procedure is beyond the scope of this paper, but can be readily found elsewhere [e.g., Refs. 2, 3]. It is worth noting that the quantified uncertainty associated with a mean stress estimate reflects a combination of numerous uncertainty sources under a statistical model used, with the major contribution from small numbers and large natural variability of stress data.

2. Models for local mean stress estimation

To facilitate demonstration of Bayesian hierarchical modelling for local mean stress estimation, the following section provides a concise and necessary introduction to the basics of hierarchical modelling and the two alternative conventional modelling approaches (i.e., no pooling and complete pooling approaches) when dealing with data which are structured in groups.

2.1. Basics

Consider a case of fitting a statistical model to multiple data groups y_j ($j = 1, 2, \dots, J$), each of which has n_j data observations y_{ij} ($i = 1, 2, \dots, n_j$) and for which group-specific model parameters θ_j are to be estimated. Note that y_{ij} denotes the i th observation in the j th data group y_j . In general, there are three types of statistical models for the analysis of such grouped data, namely no pooling, complete pooling and partial pooling (hierarchical) models. Abstract forms of the three models are illustrated by the directed graphs in Fig. 2, in which the nodes (i.e., circles) and edges (i.e., solid-line arrows) represent quantities and dependence between them, respectively.

In a no pooling model, the data of each group y_j are analysed independently to give estimation of their respective group-specific parameters θ_j with no contribution from the other groups. This is equivalent to assuming independent group-specific parameters, i.e., no similarity between them. In a complete pooling model, at the other extreme, all groups are pooled together into a single large dataset to give estimation

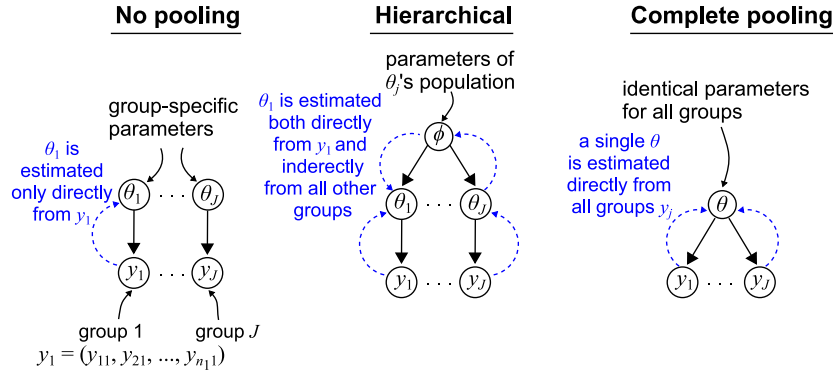


Fig. 2. Abstract forms of no pooling, hierarchical and complete pooling models (modified after^{26,33}).

of a set of common parameters θ . This implies the assumption that group-specific parameters are identical ($\theta_1 = \theta_2 = \dots = \theta$), i.e., no difference/heterogeneity between them. In practice, no pooling modelling is the usual approach to geotechnical data analysis as data from each individual site/study are usually analysed independently,^{7,9,39} and complete pooling modelling is the common approach when analysing a dataset compiled from several sites/studies.^{40–43} However, both approaches suffer from serious shortcomings in geotechnical data analysis as well as stress analysis: as the no pooling model ignores information from other sources, it may give unreliable parameter estimations when applied to a small data group; the complete pooling model is clearly inappropriate in the presence of significant between-group difference, e.g., large geological difference between sites and stress heterogeneity between locations.

Hierarchical models do not make assumptions regarding the degree of similarity between parameters θ_j of different groups (i.e., either having independent parameters as in the no pooling model or having identical parameters as in the complete pooling model); instead, it lets the data inform the similarity between group-specific parameters θ_j through assuming that θ_j 's arise from a common population distribution whose parameters ϕ are unknown. This is known as the assumption of exchangeability.^{24–26} Thus, a hierarchical model allows each individual group-specific parameter θ_j to be not only informed directly by its own data y_j , but also indirectly by the data in other groups via the assumed θ_j 's population, as illustrated in the middle graph of Fig. 2. This borrowing of information across groups is referred to as partial pooling of data, and can be thought of as a continuous generalization of the two extremes of no pooling and complete pooling which both rely on overly strict assumptions (i.e., independent and identical group-specific parameters).

The mathematical basis of the concept of partial pooling is well explained in the literature [e.g., Refs. 24–26, 44], and is briefly recounted here to provide some insights into the operation of hierarchical models. Consider a simple hierarchical model that estimates the means of J groups of normally distributed data $y_j \sim \text{Normal}(\theta_j, \sigma_j^2)$ ($j = 1, 2, \dots, J$), where the parameters of the group means θ_j are themselves assumed to follow a common normal population distribution $\theta_j \sim \text{Normal}(\mu_\theta, \sigma_\theta^2)$. For each group j , the hierarchical estimate of the group mean θ_j can be approximated as a variance-weighted average of the mean \bar{y}_j of the data in that group (i.e., the no pooling estimate of θ_j) and the mean μ_θ of θ_j 's population (i.e., the complete pooling estimate of θ_j):

$$\hat{\theta}_j^{\text{hier}} \approx \frac{\frac{n_j}{\sigma_j^2} \bar{y}_j + \frac{1}{\sigma_\theta^2} \mu_\theta}{\frac{n_j}{\sigma_j^2} + \frac{1}{\sigma_\theta^2}} = (1 - \omega_j) \bar{y}_j + \omega_j \mu_\theta, \quad (2)$$

where n_j is the number of data in group j , σ_j^2 and σ_θ^2 are the within-group variance of the data y_j in group j and the between-group variance of the group means θ_j , respectively, and

$$\omega_j = \frac{\sigma_\theta^2/n_j}{\sigma_j^2/n_j + \sigma_\theta^2} = \frac{1}{1 + n_j \sigma_\theta^2/\sigma_j^2} \quad (3)$$

is known as the ‘‘pooling factor’’ that reflects the degree of pooling of the hierarchical estimate $\hat{\theta}_j^{\text{hier}}$ of group j towards its population mean μ_θ relative to the data mean \bar{y}_j of group j on a unit scale, that is, the relative amount of information borrowed from other groups. The extreme possible values, $\omega_j = 0$ and 1, correspond to the limiting cases of no pooling ($\hat{\theta}_j^{\text{hier}} = \bar{y}_j$) and complete pooling ($\hat{\theta}_j^{\text{hier}} = \mu_\theta$), respectively.

Eqs. (2) and (3) indicate that: (i) as more data are obtained for group j (i.e., increasing sample size n_j), the pooling factor ω_j decreases and thus the hierarchical estimate $\hat{\theta}_j^{\text{hier}}$ tends to the no pooling estimate \bar{y}_j (less information from other groups); (ii) a smaller between-group variance σ_θ^2 relative to the within-group variance σ_j^2 (i.e., more similarity between groups) leads to more pooling of the hierarchical estimate towards the population mean μ_θ (i.e., more information from other groups). This explanation shows why the hierarchical model can be thought of as a continuous generalization of the two extremes of the no pooling and complete pooling models, and how it allows the parameters of each individual group to be informed indirectly by other groups.

In the context of local mean stress estimation, the use of the no pooling model and complete pooling model is equivalent to respectively assuming no similarity and no difference between the mean stress states at nearby locations. However, as noted before, our general understanding is that mean stress states at nearby locations may have, more or less, some degree of similarity, rather than being either entirely different or identical. Hence, the more suitable hierarchical model may be used, as it allows for accommodation of the possible similarity between mean stress states at nearby locations and may thereby achieve borrowing of information across stress data groups from nearby locations.

2.2. No pooling model

Using a no pooling model, stress data from each location are analysed independently to estimate the mean stress state at that location, and this is how stress data are customarily analysed in practice. In a previous work by the authors, a basic Bayesian multivariate normal (MVN) model was proposed for local mean stress estimation and uncertainty quantification given a stress data group measured within a local rock volume.²⁰ In the context of multiple nearby locations, the no pooling model is simply a separate application of the basic Bayesian MVN model to the stress data group from each location and its likelihood function for group j is given in a compact form as

$$s_{ij} \sim \text{MVN}(\boldsymbol{\mu}_j, \boldsymbol{\Sigma}), \quad (4)$$

where $s_{ij} = [\sigma_{x(ij)} \ \tau_{xy(ij)} \ \tau_{xz(ij)} \ \sigma_{y(ij)} \ \tau_{yz(ij)} \ \sigma_{z(ij)}]^T \in \mathbb{R}^6$ denotes the i th measured vector of the six distinct stress tensor components at location j defined in a common x - y - z Cartesian coordinate system of x East, y North and z vertically upwards, and $\boldsymbol{\mu}_j = [\mu_{\sigma_x(j)} \ \mu_{\tau_{xy}(j)} \ \mu_{\tau_{xz}(j)} \ \mu_{\sigma_y(j)} \ \mu_{\tau_{yz}(j)} \ \mu_{\sigma_z(j)}]^T \in \mathbb{R}^6$ and $\boldsymbol{\Sigma} \in \mathbb{R}^{6 \times 6}$ is the mean stress vector of interest and the covariance matrix representing

the stress variability for location j , respectively. Note that here we assumed a common covariance matrix Σ for all locations instead of location-specific covariance matrices, given that only local mean stress is of interest in this paper and also stress data measured at a location are sometimes less than the required number (at least 7) for robust estimation of a 6×6 covariance matrix.¹⁶

Throughout this paper, we write the likelihood function in a compact form as Eq. (4) to avoid its explicit multiplicative form of the probability density function of the MVN distribution that may overwhelm the readers like:

$$p(s_{1j}, \dots, s_{n_{jj}} | \boldsymbol{\mu}_j, \Sigma) = \prod_{i=1}^{n_{jj}} (2\pi)^{-3} \sqrt{|\Sigma|} \exp\left(-\frac{1}{2} (s_{ij} - \boldsymbol{\mu}_j)^\top \Sigma^{-1} (s_{ij} - \boldsymbol{\mu}_j)\right) \quad (5)$$

Here, to reflect a lack of prior knowledge about the specific values of parameters, we assign weakly informative priors to the parameters $\boldsymbol{\mu}_j$ and Σ . For the mean vector $\boldsymbol{\mu}_j$ of a MVN distribution, a common prior choice is the multivariate normal distribution with hyperparameters of mean vector $\boldsymbol{\mu}_0 \in \mathbb{R}^6$ and covariance matrix $\Sigma_0 \in \mathbb{R}^{6 \times 6}$. To express our weak prior knowledge that the values of the normal (i.e., $\mu_{\sigma_x(j)}$, $\mu_{\sigma_y(j)}$ and $\mu_{\sigma_z(j)}$) and shear (i.e., $\mu_{\tau_{xy}(j)}$, $\mu_{\tau_{xz}(j)}$ and $\mu_{\tau_{yz}(j)}$) components of the mean stress vector $\boldsymbol{\mu}_j$ respectively most likely (with roughly 0.95 probability) fall between 10 ± 50 MPa and 0 ± 15 MPa, we set $\boldsymbol{\mu}_0 = [10 \ 0 \ 0 \ 10 \ 0 \ 10]^\top$ MPa with a vector of variances to be $(25^2, 7.5^2, 7.5^2, 25^2, 7.5^2, 25^2)$ MPa for $\boldsymbol{\mu}_j$'s components and zero covariance between these components, as follows:

$$\boldsymbol{\mu}_j \sim \text{MVN}(\boldsymbol{\mu}_0 = [10 \ 0 \ 0 \ 10 \ 0 \ 10]^\top \text{ MPa}, \Sigma_0 = \text{diag}(25^2, 7.5^2, 7.5^2, 25^2, 7.5^2, 25^2) \text{ MPa}^2), \quad (6)$$

where $\text{diag}(\cdot)$ is the diagonal matrix operator.

For the prior choice for covariance matrix Σ , it is advocated to decompose it into a vector of six standard deviations $\boldsymbol{\zeta} \in \mathbb{R}^6$ and a correlation matrix $\Omega \in \mathbb{R}^{6 \times 6}$, and such a decomposition allows us to specify separate priors for the correlation matrix and each standard deviation component, thereby giving us the flexibility to better express prior information.^{24,28,45} For each standard deviation of $\boldsymbol{\zeta}$, a normal distribution with mean 0 MPa and standard deviation 5 MPa truncated below 0 is specified to express our only weak prior knowledge about its value; that is, the standard deviation associated with each stress tensor component will most likely lie between 0 and 10 MPa (with approximately 0.95 probability). For the prior choice for correlation matrix Ω , the LKJ distribution, named after the authors in Ref. 46, is recommended to be used as the default.^{24,28,47,48} The LKJ distribution can be considered as a multivariate generalization of the symmetric beta distribution, and is expressed by a single shape parameter $\eta > 0$. For example, for $\eta = 1$, the marginal probability density is uniform between -1 and 1 for all correlation components, and with larger η the marginal density increasingly concentrates around 0 and therefore the correlation matrix tends to the identity matrix. For more details on prior choice for covariance matrix as well as the LKJ distribution, we refer the interested readers to the works.^{20,24,28,46,47} Here, a LKJ distribution with a small shape parameter $\eta = 5$ is assigned to the correlation matrix Ω to reflect a lack of prior knowledge about the specific values of the correlations between the six distinct stress tensor components. The weakly informative priors for Σ discussed above are summarized as follows:

$$\begin{aligned} \Sigma &= \text{diag}(\boldsymbol{\zeta})\Omega \text{diag}(\boldsymbol{\zeta}) \\ \boldsymbol{\zeta} &\sim \text{Normal}(0, 5^2) \text{ MPa, truncated below 0.} \\ \Omega &\sim \text{LKJ}(\eta = 5) \end{aligned} \quad (7)$$

2.3. Complete pooling model

The complete pooling model is the application of a statistical model (i.e., the basic Bayesian MVN model herein) to the combined stress

data from all nearby locations under consideration, implying the assumption that these locations have an identical local mean stress state $\boldsymbol{\mu}$. This is generally an unrealistic assumption as stresses often display natural variability, even in a small domain.^{2,49-52} Notwithstanding being uncommon in local mean stress estimation, in this paper the complete pooling model is briefly demonstrated in comparison with the customary no pooling model and the proposed hierarchical model in order to statistically emphasize its inappropriateness. The likelihood function of the complete pooling model is written as

$$s_{ij} \sim \text{MVN}(\boldsymbol{\mu}, \Sigma), \quad (8)$$

and the weakly informative priors for $\boldsymbol{\mu}$ and Σ are

$$\begin{aligned} \boldsymbol{\mu} &\sim \text{MVN}(\boldsymbol{\mu}_0 = [10 \ 0 \ 0 \ 10 \ 0 \ 10]^\top \text{ MPa}, \\ \Sigma_0 &= \text{diag}(25^2, 7.5^2, 7.5^2, 25^2, 7.5^2, 25^2) \text{ MPa}^2) \end{aligned} \quad (9)$$

and

$$\begin{aligned} \Sigma &= \text{diag}(\boldsymbol{\zeta})\Omega \text{diag}(\boldsymbol{\zeta}) \\ \boldsymbol{\zeta} &\sim \text{Normal}(0, 5^2) \text{ MPa, truncated below 0.} \\ \Omega &\sim \text{LKJ}(\eta = 5) \end{aligned} \quad (10)$$

2.4. Hierarchical model

Assuming either entirely different or identical mean stress states at nearby locations is both overly strict and potentially unreasonable. Instead, it is more reasonable to only recognize that nearby local mean stress states may have some degree of similarity. The hierarchical model accommodates such possible similarity by assuming that nearby mean stress states $\boldsymbol{\mu}_j$ arise from a common population distribution, as previously illustrated in the middle graph of Fig. 2. This assumption of exchangeability is the essence of the hierarchical model that allows borrowing of information across stress data from nearby locations; that is, each location-specific mean stress vector $\boldsymbol{\mu}_j$ is not only informed directly by the stress data of location j itself but also informed indirectly by the data of all other locations. The likelihood function of the hierarchical model can be expressed as

$$s_{ij} \sim \text{MVN}(\boldsymbol{\mu}_j, \Sigma), \quad (11)$$

where Σ is assigned the same weakly informative priors as the no pooling and complete pooling models as

$$\begin{aligned} \Sigma &= \text{diag}(\boldsymbol{\zeta})\Omega \text{diag}(\boldsymbol{\zeta}) \\ \boldsymbol{\zeta} &\sim \text{Normal}(0, 5^2) \text{ MPa, truncated below 0.} \\ \Omega &\sim \text{LKJ}(\eta = 5) \end{aligned} \quad (12)$$

Here, a MVN prior distribution is assumed for $\boldsymbol{\mu}_j$'s to accommodate their potential similarity and is written as

$$\boldsymbol{\mu}_j \sim \text{MVN}(\boldsymbol{\mu}_0, \Sigma_0), \quad (13)$$

and the hyper-parameters $\boldsymbol{\mu}_0$ and Σ_0 are then assigned weakly informative priors as:

$$\begin{aligned} \boldsymbol{\mu}_0 &\sim \text{MVN}([10 \ 0 \ 0 \ 10 \ 0 \ 10]^\top \text{ MPa}, \\ &\text{diag}(25^2, 7.5^2, 7.5^2, 25^2, 7.5^2, 25^2) \text{ MPa}^2) \end{aligned} \quad (14)$$

and

$$\begin{aligned} \Sigma_0 &= \text{diag}(\boldsymbol{\zeta}_0)\Omega_0 \text{diag}(\boldsymbol{\zeta}_0) \\ \boldsymbol{\zeta}_0 &\sim \text{Normal}(0, 5^2) \text{ MPa, truncated below 0.} \\ \Omega_0 &\sim \text{LKJ}(\eta = 5) \end{aligned} \quad (15)$$

Note that in Bayesian inference, there always exist alternative formulations of prior distributions in terms of the choice of the distribution type and the values of the priors' parameters, and here we only need to ensure that the employed priors serves the purpose of generally allowing the data to dominate the posterior inferences. An informal prior sensitivity analysis, not reported here for brevity, shows that the weakly informative priors employed in this paper have served their intended purpose. In fact, prior sensitivity analysis is essential to any rigorous Bayesian analysis but is often overlooked in the literature.

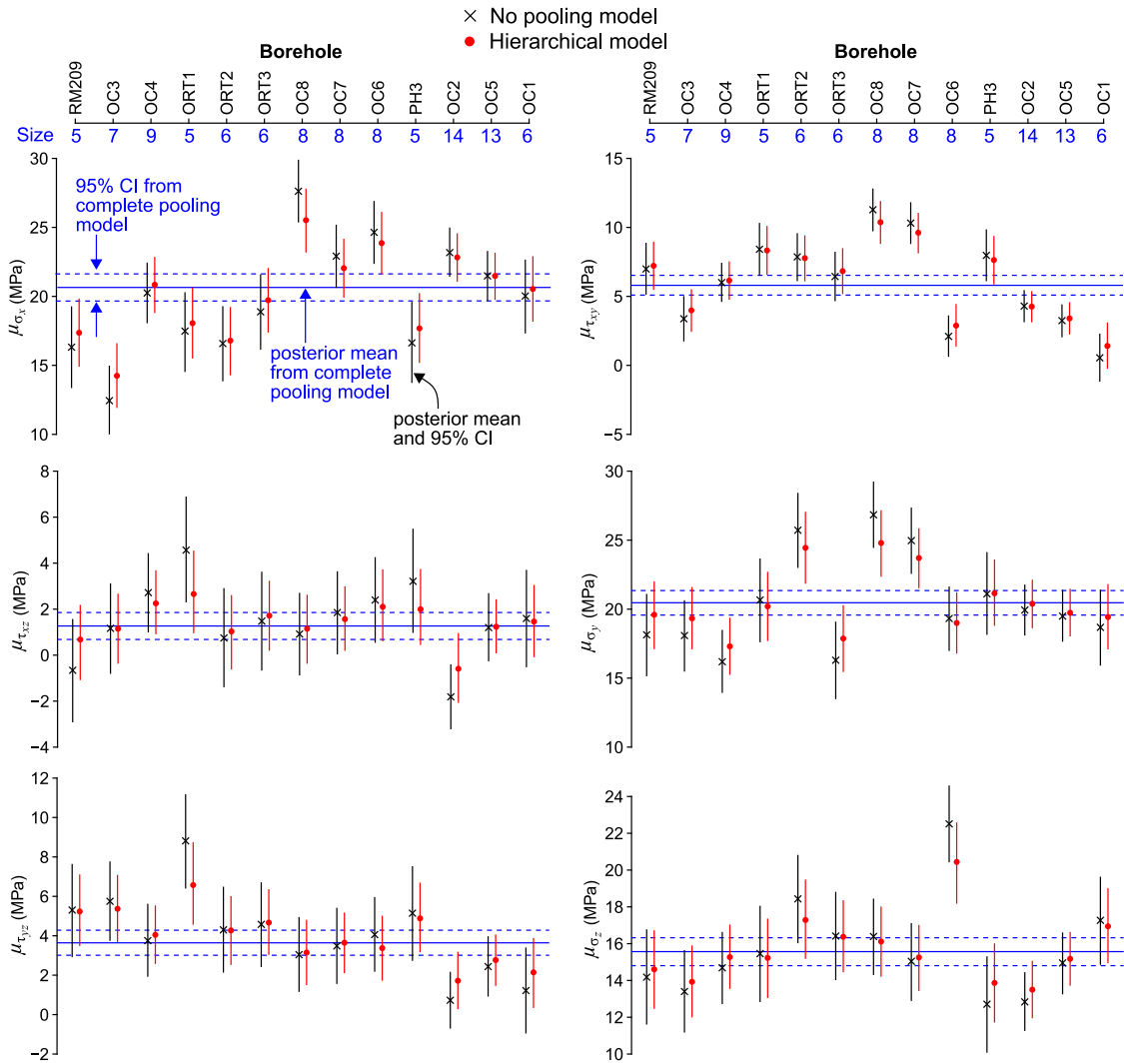


Fig. 3. Posterior estimates of the mean stress vector for each borehole.

3. Application

3.1. Data and Bayesian computation

To demonstrate the three Bayesian models in question for local mean stress estimation, the 100 high-quality stress tensors measured from 13 nearby boreholes on the 240 level of the AECL’s URL (referred to as URL240 hereafter, see Fig. 1) are used as a study example in this paper, and these stress data are given in Appendix A.

All Bayesian models in this paper were fitted using the modern Bayesian inference program Stan⁴⁸ in conjunction with the programming language R.⁵³ Stan provides two Markov chain Monte Carlo (MCMC) simulation methods to implement Bayesian posterior sampling, namely, the Hamiltonian Monte Carlo (HMC) algorithm and its adaptive variant the No-U-Turn sampler (NUTS). A detailed introduction to these MCMC algorithms is beyond the scope of this paper but can be readily found elsewhere [e.g., Refs. 54–56]. Appendix B provides the Stan codes of the Bayesian hierarchical MVN model of Eqs. (11)–(15). Three Markov chains with different initial values were run in parallel to examine their convergence, and a total of 9000 posterior draws (i.e., 3000 draws per chain) were simulated to approximate the posterior distribution of each parameter which are used for further inference (e.g., posterior mean and 95% credible interval).

3.2. Estimation of the mean stress vectors

Fitting the three models in question to the URL240 dataset, Fig. 3 shows the posterior means and the associated 95% credible intervals (95% CIs) of the six components of the mean stress vector (i.e., μ_{σ_x} , $\mu_{\tau_{xy}}$, $\mu_{\tau_{xz}}$, μ_{σ_y} , $\mu_{\tau_{yz}}$ and μ_{σ_z}) for each of the 13 boreholes. Note that for a given parameter, the posterior mean can be taken as the point estimate, and the 95% CI represents the uncertainty associated with the estimate and can be directly interpreted as an interval containing the true value of the parameter with 0.95 probability.²⁴

We first briefly demonstrate why the complete pooling model is inappropriate for local mean stress estimation. The posterior means and 95% CIs obtained from the complete pooling model are shown respectively by the blue solid and dashed lines that traverse each subfigure of Fig. 3. Given that the complete pooling model uses combined stress data from multiple borehole locations to estimate a single mean stress vector, it expectedly yields less uncertain estimates for the six mean stress components than those obtained from the no pooling model, as indicated by the narrower 95% CIs. Despite being desirable at first sight, these complete pooling estimates are misleading in that their 95% CIs fails to capture the no pooling estimates of many individual boreholes. For instance, 10 out of the 13 no pooling μ_{σ_x} estimates fall outside the complete pooling 95% CI. This observation suggests that the complete pooling estimates are not well representative of the mean stress state at each borehole location and thus statistically confirms

the inappropriateness of the complete pooling model for mean stress estimation at the borehole scale. The reason behind this was noted previously, that is, the complete pooling model ignores the variation of mean stress states between locations, yet stresses often display significant variability in nature.

Now we discuss how application of the hierarchical model can improve local mean stress estimation from the no pooling model that is customarily used in practice. Fig. 3 shows that for each borehole, the hierarchical model yields a different but generally more certain estimate of the mean stress vector than does the no pooling model, as indicated by the narrower hierarchical 95% CIs in varying degrees for all six mean stress components. As an example, for borehole RM209, the no pooling model yields a point estimate of μ_{σ_x} of around 16.32 MPa accompanied by a 95% CI of (13.40, 19.23) MPa, while the hierarchical model gives a more certain μ_{σ_x} estimate of 17.36 MPa with a narrower 95% CI of (14.94, 19.80) MPa; such more or less uncertainty reduction is also observed for the other five mean stress components (i.e., $\mu_{\tau_{xy}}$, $\mu_{\tau_{xz}}$, μ_{σ_y} , $\mu_{\tau_{yz}}$ and μ_{σ_z}) for the same borehole.

To give a better sense of how the overall uncertainty in the estimated mean stress vector is reduced for each borehole by hierarchical modelling, here we employ a widely used scalar measure of multivariate dispersion called “effective variance” to quantify the overall dispersion of the joint posterior distribution of the six mean stress components.^{57,58} For a multivariate data distribution of dimension p , the effective variance is defined as $V_e = |\Sigma|^{1/p}$, where Σ is the covariance matrix of the data distribution and $|\cdot|$ denotes the matrix determinant. Hence, the effective variance for the mean stress vector μ is calculated as the 6th root of the determinant of the covariance matrix of μ 's posterior distribution. Fig. 4 illustrates the effective variance for the mean stress vector of each borehole estimated from the no pooling and hierarchical models, respectively represented by black crosses and red solid circles. This figure clearly shows different degrees of reduction in the effective variance (i.e., overall uncertainty) of the estimated mean stress vector for the 13 boreholes when applying the hierarchical model. For example, application of the hierarchical model leads to a noticeable reduction in the effective variance of the mean stress estimate from 1.27 MPa² to 0.88 MPa² for borehole RM209, and a slight reduction from 0.51 MPa² to 0.46 MPa² for borehole OC2. Fig. 4 also shows that smaller stress groups generally exhibit more overall uncertainty reduction in their mean stress estimates compared to stress groups with larger sizes, indicating that more information is borrowed from other stress groups under the hierarchical model. This phenomenon is previously explained by Eqs. (2) and (3).

The results shown in both Figs. 3 and 4 demonstrate that compared to the customary no pooling model, the proposed hierarchical model is able to improve local mean stress estimation simultaneously at each borehole location by allowing information to be borrowed across stress data from these nearby boreholes.

3.3. Estimation of the principal mean stresses

In earth sciences, stress state is commonly of particular interest in terms of principal stresses. Here, we refer to principal stress associated with the mean stress tensor as principal mean stress, and denote it as μ_σ hereafter. Hence, in the following we show how the hierarchical model may improve the customary no pooling estimation of the principal mean stress state for each borehole. In the Bayesian framework, the MCMC simulation provides a straightforward means of computing the posterior distribution of the principal mean stress μ_σ by transformation of the posterior distribution of the associated mean stress vector μ . The approach is as follows: for each posterior draw of μ , the eigenvalues and eigenvectors of its associated stress tensor are calculated to give one posterior draw of μ_σ magnitudes and orientations, respectively; repeating this procedure for each posterior draw of μ gives the posterior distributions of μ_σ magnitudes and orientations, with the posterior estimates then being determined from them.^{20,23,59}

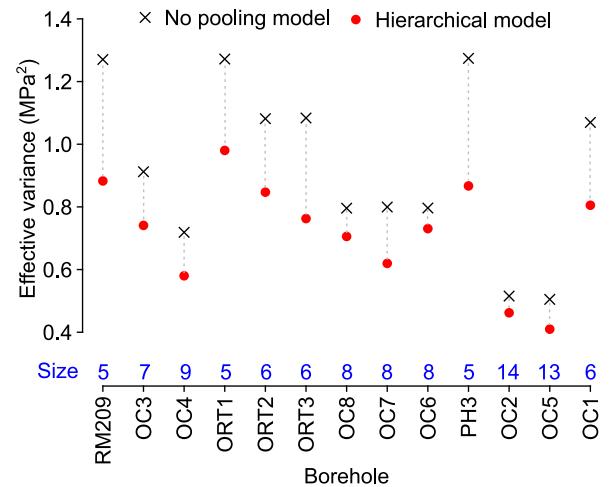


Fig. 4. Effective variance (overall uncertainty) reduction for the mean stress vector at each borehole resulting from the hierarchical model.

Following the approach described above, we obtain the posterior estimates of the magnitudes and orientations of the three principal mean stress components (i.e., μ_{σ_1} , μ_{σ_2} and μ_{σ_3}) for the 13 boreholes in question resulting from the no pooling and hierarchical models, as depicted in Figs. 5 and 6. The posterior estimates of the principal mean stress orientations are displayed using equal-angle lower hemispherical projections. For clarity and easier comparison, each hemispherical projection has been rotated to place the no pooling posterior mean orientation of one principal mean stress component at the centre of the projection, and the no pooling posterior mean orientations of the other two principal mean stress components at the top, bottom, left and right positions. Similar to 95% CIs, 95% credible regions (CRs) marked by closed curves delineate the plausible regions within which the principal mean stress orientations will lie with 0.95 probability. Further owing to the space constraint, only the principal mean stress orientation estimates for boreholes OC1 and PH3 are displayed in Fig. 6.

As expected, Figs. 5 and 6 show that application of the hierarchical model generally leads to different degrees of uncertainty reduction for both the magnitude and orientation estimates of the three principal mean stress components for each borehole. For example, for borehole OC1, the hierarchical model gives a best estimate of μ_{σ_1} magnitude of 22.6 MPa with a narrower 95% CI of (20.2, 25.7) MPa compared to the 95% CI of (18.9, 24.9) MPa for the no pooling estimate of 21.2 MPa, and gives a best estimate of μ_{σ_1} orientation of 230/24 (trend/plunge) with a 95% CR that is substantially smaller than that associated with the no pooling estimate of 244/27. These observations again demonstrate that the proposed hierarchical model is capable of improving the mean stress estimation in terms of both principal stress magnitudes and orientations simultaneously for each borehole.

4. A simulation study

In this section, we carry out a simulation study to further demonstrate the advantages of the hierarchical model using simulated stress data, particularly the flexibility of the hierarchical model as a continuous generalization of the no pooling and complete pooling models.

4.1. Data generation

We simulate multiple stress data groups corresponding to multiple locations from the hierarchical model, i.e., $\mu_j \sim \text{MVN}(\mu_0, \Sigma_0)$ and $s_{ij} \sim \text{MVN}(\mu_j, \Sigma)$ with assumed values for parameters μ_0 , Σ_0 and Σ . The stress data simulation process commences with simulating a

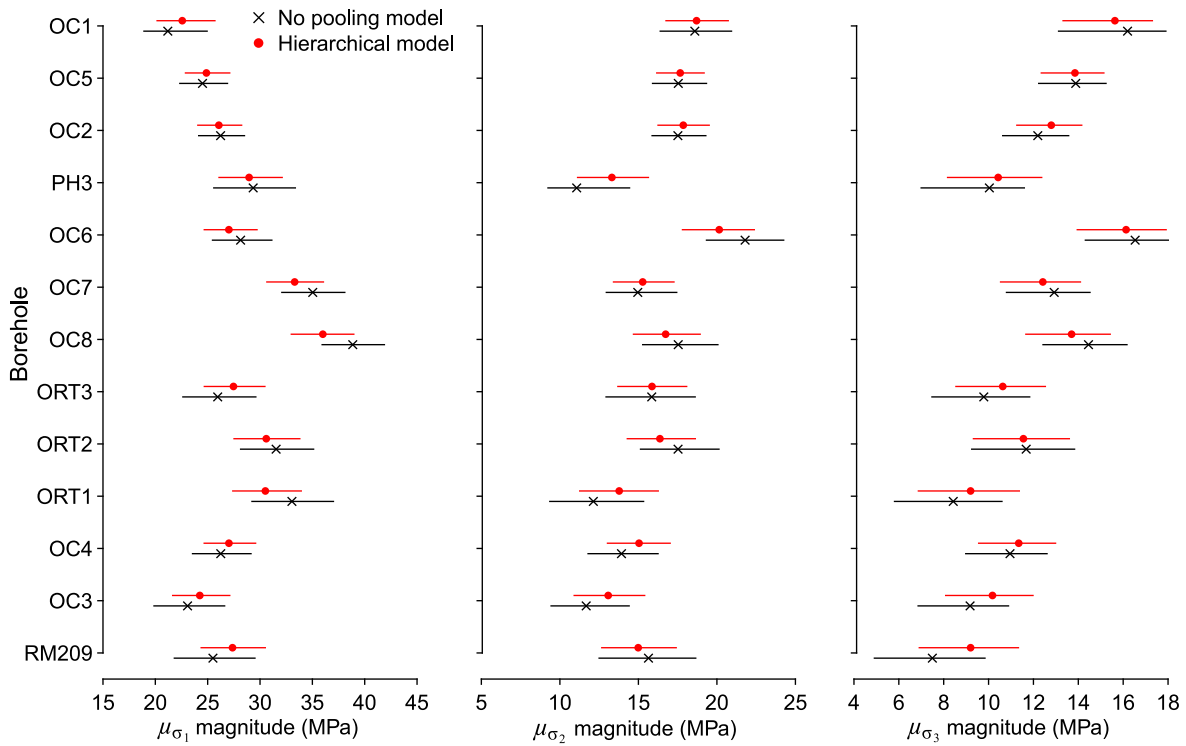


Fig. 5. Posterior estimates of the principal mean stress magnitudes for each borehole.

Table 1
Parameter values of the three simulation scenarios.

$\boldsymbol{\mu}_0$ (MPa)	Σ_0 (MPa ²)	Σ (MPa ²)
$[20 \ 5 \ -1 \ 15 \ 2 \ 10]^\top$	$25 \times \Sigma$	$\text{diag}(2^2, 1^2, 1^2, 2^2, 1^2, 2^2)$
$[20 \ 5 \ -1 \ 15 \ 2 \ 10]^\top$	$1/5 \times \Sigma$	$\text{diag}(2^2, 1^2, 1^2, 2^2, 1^2, 2^2)$
$[20 \ 5 \ -1 \ 15 \ 2 \ 10]^\top$	$1/25 \times \Sigma$	$\text{diag}(2^2, 1^2, 1^2, 2^2, 1^2, 2^2)$

mean stress vector $\boldsymbol{\mu}_j$ for location j from $\boldsymbol{\mu}_j$'s MVN population given $\boldsymbol{\mu}_0$ and Σ_0 , followed by generating a group of stress vector data s_{ij} for location j from the MVN stress distribution given $\boldsymbol{\mu}_j$ and Σ . Here, we consider three simulation scenarios for the assumed parameter values, as summarized in Table 1.

The covariance matrix Σ_0 and Σ respectively represents between-location variation and within-location variation in the stress data, and hence the three scenarios correspond to three different levels of between-location similarity, i.e., little, moderate and high between-location similarity. For each scenario, 10 stress data groups of a common group size of 8 (i.e., $j = 1, 2, \dots, 10$ and $i = 1, 2, \dots, 8$) were simulated and then used to fit the three models (i.e., the no pooling, complete pooling and hierarchical models) given in Section 2. From the simulation results, pooling factors and effective variances are calculated for comparison between the three simulation scenarios. Note that the purpose of the simulation study is merely to use different stress data to further demonstrate the advantages of the proposed hierarchical model in local mean stress estimation, so neither different assumed parameter values nor different numbers and sizes of stress data groups are considered here.

4.2. Simulation results

Fig. 7 illustrates the pooling factor of the hierarchical mean stress estimate associated with each group for each of the three simulation scenarios. As noted in Section 2.1, the pooling factor of the hierarchical estimate of one group can be interpreted as a measure of the amount of information borrowed from other groups relative to that group's own

information on a unit scale ranging from no pooling to complete pooling. It is seen in Fig. 7 that when increasing between-group similarity (from simulation scenario 1 to 3), each group expectedly borrows more information from other groups relative to its own, thereby leading to more pooling of the hierarchical mean stress estimates indicated by increasingly larger pooling factors. It is noteworthy that for simulation scenario 1, the pooling factors of the 10 stress groups are all close to 0, indicating that the hierarchical model tends to the no pooling model when there is little similarity between stress data groups. Fig. 8 depicts the effective variance (overall uncertainty) reduction for the mean stress estimate of each group between the no pooling and hierarchical models for each of the three simulation scenarios. Apparently, as more similarity between stress data groups are present, the hierarchical model is able to borrow more information across groups accordingly (larger pooling factors) and hence generally leads to more reduction in the overall uncertainty in the mean stress estimates.

This simple simulation study above again demonstrate the hierarchical model can give improved local mean stress estimation simultaneously for each of the nearby locations than does the customary no pooling model. More importantly, it confirms that the hierarchical model is indeed a generalization of the conventional no pooling and complete pooling models which both involve extreme assumptions regarding the level of between-group similarity, and provides a flexible framework that allows simultaneous and adaptive borrowing of information across stress data from nearby locations via accommodating possible between-location similarity. For these reasons, the hierarchical model should be preferred for local mean stress estimation when stress data from multiple nearby locations are available.

5. Discussion

Local mean stress is an important input parameter to many applications in rock mechanics and geomechanics. We have demonstrated that given a number of stress data groups measured from nearby locations, the Bayesian hierarchical model developed in this paper is able to both quantify probabilistically and reduce uncertainty in the estimated mean

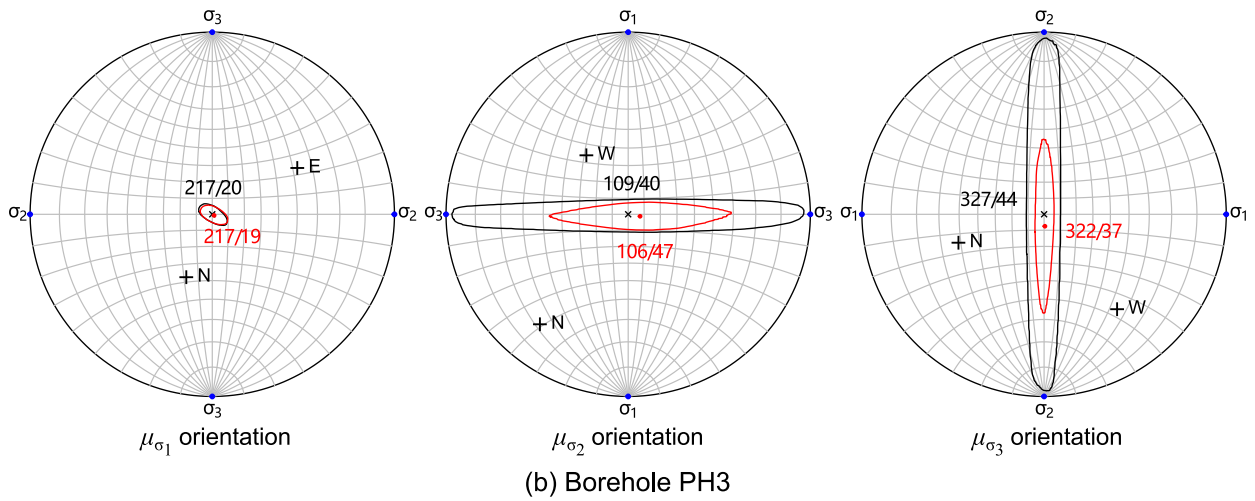
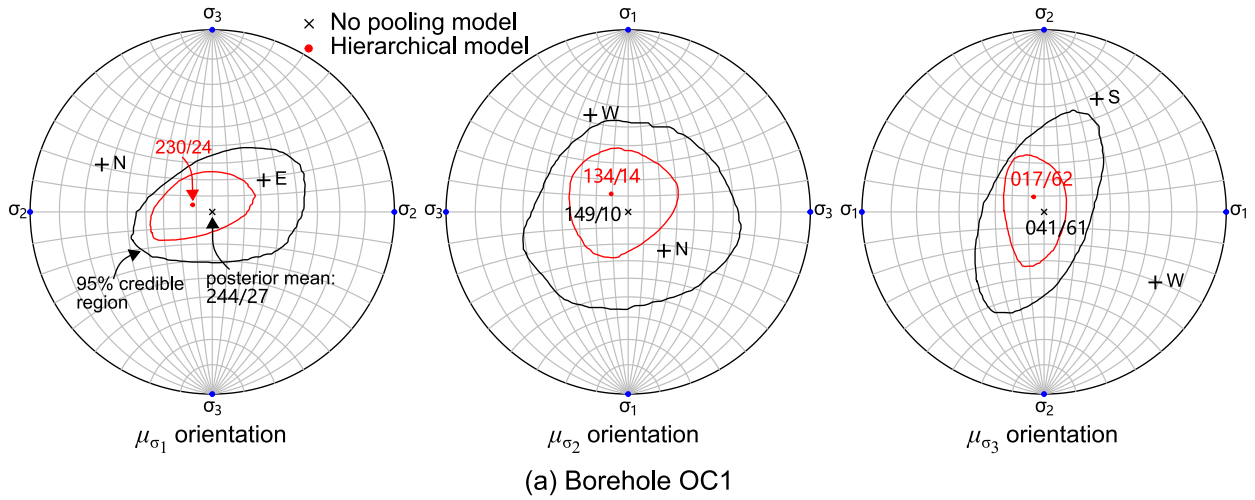


Fig. 6. Posterior estimates of the principal mean stress orientations for boreholes OC1 and PH3.

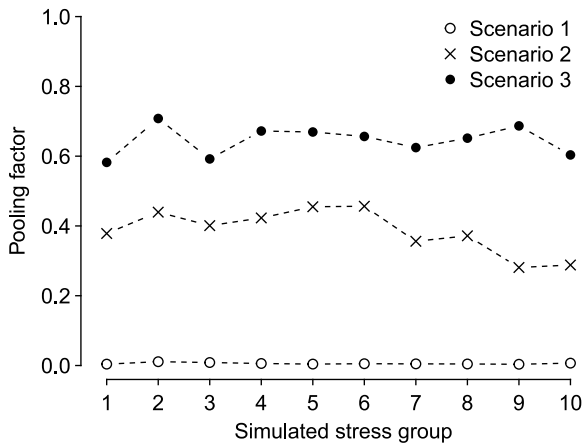


Fig. 7. Pooling factors of the hierarchical estimates for the three simulation scenarios.

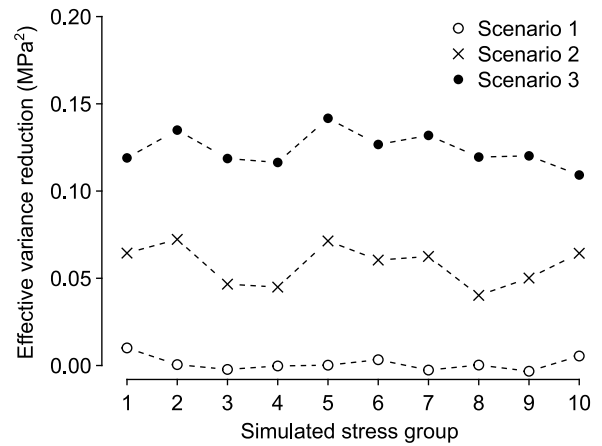


Fig. 8. Effective variance reduction from the no pooling to the hierarchical model for the three simulation scenarios.

stress state for each location through borrowing information across stress data from nearby locations. Such abilities are particularly important when facing limited stress measurement data and/or significant natural stress variability in a local volume. Moreover, probabilistic uncertainty quantification and reduction in mean stress estimation not only permits probabilistic implementation of further analyses in other

applications involving mean stresses, but also gives more accurate analysis results.

In this paper, we used weakly informative priors to demonstrate how the Bayesian hierarchical model allows information to be borrowed across stress data from nearby locations. This hierarchical model may be extended to incorporate other available stress information

Table A.1

In situ stress tensors measured on the URL's 240 level interpreted using the anisotropic model [from Ref. 9].

No.	Stress tensor components (MPa)						Borehole	No.	Stress tensor components (MPa)						Borehole
	σ_x	τ_{xy}	τ_{xz}	σ_y	τ_{yz}	σ_z			σ_x	τ_{xy}	τ_{xz}	σ_y	τ_{yz}	σ_z	
1	17.25	8.11	-0.44	19.27	5.48	13.08	RM209	51	22.38	9.94	3.77	27.41	3.78	18.72	OC7
2	14.31	5.66	-0.76	18.12	5.13	15.97	RM209	52	19.61	8.41	1.42	18.64	5.34	12.05	OC7
3	15.63	7.39	-0.60	17.22	6.36	9.95	RM209	53	20.39	8.97	4.29	23.74	5.67	17.46	OC7
4	18.45	7.96	-1.06	20.59	5.02	16.26	RM209	54	25.35	10.29	0.25	22.21	4.00	15.35	OC7
5	16.35	6.43	-0.28	16.40	5.23	15.65	RM209	55	17.24	3.61	4.45	15.69	4.44	18.16	OC6
6	10.93	3.19	1.95	15.58	6.97	13.40	OC3	56	22.06	3.45	3.20	18.24	4.07	17.89	OC6
7	12.19	0.79	3.62	17.28	-0.14	13.73	OC3	57	26.49	0.67	3.52	20.89	5.07	23.83	OC6
8	14.22	3.89	1.04	19.29	7.37	15.29	OC3	58	20.91	-1.77	2.63	17.66	3.95	24.23	OC6
9	10.47	0.72	2.35	18.64	8.58	15.60	OC3	59	29.70	4.58	3.09	24.08	7.20	24.12	OC6
10	12.83	6.88	-0.57	19.74	5.08	10.03	OC3	60	21.18	0.65	4.46	16.65	3.85	23.48	OC6
11	12.58	3.73	-0.49	19.80	7.01	13.03	OC3	61	32.41	1.02	2.45	21.83	5.31	31.56	OC6
12	14.17	4.72	0.58	16.89	6.24	12.94	OC3	62	27.52	4.79	-4.22	20.21	-0.70	17.17	OC6
13	13.12	0.68	3.80	9.66	4.80	21.03	OC4	63	16.10	7.99	3.39	19.43	4.28	11.97	PH3
14	19.35	-3.13	-3.62	7.27	-1.36	10.38	OC4	64	16.71	7.04	3.38	21.10	5.95	13.39	PH3
15	16.97	4.38	6.28	14.61	6.08	15.92	OC4	65	16.20	8.44	3.35	20.82	4.84	11.38	PH3
16	21.17	7.00	5.69	18.26	5.38	15.77	OC4	66	16.60	7.91	2.88	23.55	6.26	12.45	PH3
17	22.55	7.56	7.05	20.85	6.51	15.40	OC4	67	18.04	9.18	3.65	21.66	5.11	14.40	PH3
18	29.16	8.50	4.67	17.95	5.14	15.79	OC4	68	21.35	4.20	2.48	21.44	2.64	12.01	OC2
19	15.03	9.38	3.86	19.69	6.95	10.78	OC4	69	30.08	4.35	-8.61	24.60	13.39	18.13	OC2
20	24.99	8.87	-6.24	17.87	-4.50	12.85	OC4	70	31.77	2.28	0.10	27.69	0.69	15.84	OC2
21	20.29	11.23	3.42	20.25	5.32	14.36	OC4	71	20.62	4.08	0.81	15.15	-2.26	5.93	OC2
22	15.90	8.10	1.26	17.40	10.27	13.50	ORT1	72	21.61	4.89	-2.39	20.26	-1.27	13.12	OC2
23	16.54	9.59	9.24	27.84	9.52	12.92	ORT1	73	22.42	3.77	1.96	20.67	3.16	12.41	OC2
24	19.11	9.12	4.17	21.58	8.02	17.91	ORT1	74	23.14	5.29	-4.11	18.69	-2.16	15.38	OC2
25	18.01	7.79	3.30	19.88	8.08	17.11	ORT1	75	22.50	3.04	-4.83	17.66	-2.50	14.84	OC2
26	18.22	8.12	5.71	17.72	9.49	16.06	ORT1	76	21.57	5.36	0.00	20.16	1.06	11.07	OC2
27	16.50	7.86	1.84	26.27	7.13	18.73	ORT2	77	18.93	3.01	3.48	18.84	3.98	13.83	OC2
28	21.10	10.96	-0.83	32.78	2.30	22.52	ORT2	78	24.52	4.71	-3.55	20.33	-1.77	11.65	OC2
29	17.19	8.65	1.72	25.55	5.39	16.26	ORT2	79	21.67	3.91	-6.82	16.36	-2.65	16.67	OC2
30	13.11	7.78	0.18	22.04	0.74	17.05	ORT2	80	21.34	5.35	-2.11	18.64	-1.27	10.92	OC2
31	18.36	6.74	0.63	26.89	2.90	19.86	ORT2	81	23.37	6.38	-2.05	19.16	-0.78	7.87	OC2
32	13.73	5.84	1.29	21.73	7.95	16.34	ORT2	82	23.60	5.95	-0.52	21.47	-0.25	11.82	OC5
33	17.55	7.91	1.06	18.55	5.87	16.40	ORT3	83	12.95	-2.37	-4.16	13.21	5.39	22.04	OC5
34	20.35	6.26	1.07	14.71	2.74	16.95	ORT3	84	24.31	4.46	1.28	21.27	0.14	15.02	OC5
35	21.37	6.62	1.64	17.98	3.97	17.65	ORT3	85	21.81	2.38	3.42	19.53	3.42	15.76	OC5
36	19.89	5.80	1.36	14.96	4.39	16.05	ORT3	86	20.03	1.10	3.45	20.12	4.42	19.76	OC5
37	17.88	7.59	2.17	17.56	5.99	14.76	ORT3	87	21.59	2.73	3.11	19.77	3.90	16.34	OC5
38	16.77	4.97	1.89	14.81	5.20	16.81	ORT3	88	22.08	4.76	1.70	21.08	2.87	13.24	OC5
39	25.86	12.95	1.69	30.03	2.38	17.12	OC8	89	20.43	5.08	0.71	17.36	1.64	12.31	OC5
40	30.38	10.51	2.18	26.96	3.40	18.05	OC8	90	20.44	5.29	-2.36	15.34	-3.12	8.52	OC5
41	29.08	11.67	-0.23	27.10	2.53	15.62	OC8	91	19.78	4.08	2.73	18.78	1.94	12.25	OC5
42	29.63	12.02	0.83	31.00	5.97	17.37	OC8	92	21.66	4.76	0.43	19.10	1.31	11.75	OC5
43	27.95	13.63	2.82	34.00	4.81	17.34	OC8	93	24.06	2.66	2.99	22.89	4.65	17.34	OC5
44	26.38	9.90	1.31	22.87	3.61	17.46	OC8	94	26.90	1.64	3.19	24.10	5.83	18.30	OC5
45	26.63	9.39	0.19	20.47	1.69	14.41	OC8	95	23.60	3.76	2.71	14.13	1.14	14.87	OC1
46	25.73	11.18	-1.07	23.61	0.44	13.67	OC8	96	15.98	-0.74	0.04	16.41	1.27	17.52	OC1
47	25.31	12.46	2.53	28.86	3.05	15.33	OC7	97	15.55	1.59	1.83	16.92	0.28	16.83	OC1
48	28.59	11.95	2.00	29.86	4.36	16.55	OC7	98	18.91	-0.55	2.04	20.50	1.23	19.39	OC1
49	22.98	11.31	-2.84	29.74	-0.14	14.18	OC7	99	23.84	0.25	1.03	21.72	1.24	15.65	OC1
50	19.36	10.06	3.82	20.45	2.32	10.59	OC7	100	22.65	-0.91	2.17	22.85	2.46	19.50	OC1

sources (see Section 1) in form of informative prior distributions, and may thus further improve mean stress estimation. In this respect, the Bayesian hierarchical model can be thought of as a general and powerful framework that allows stress information from different sources to be logically integrated for mean stress estimation. However, many challenges are present in developing informative priors from stress information sources, and the three key ones were already discussed elsewhere^{20,23} but are reiterated here for emphasis as follows.

First, development of informative priors requires sound knowledge of both geology and rock mechanics in order to identify valid stress information corresponding to each individual source, and also sufficient knowledge of probability and statistics to formulate appropriate probability distributions to express such information. Second, when multiple pieces of additional information on the same stress components are available (e.g., borehole breakouts and hydraulic fracturing both inform the orientation of σ_1), information aggregation is needed for which the issues of compatibility between and relative weighting of pieces of information must be considered. Third, many sources of stress information are present in terms of principal stresses, and so the

Bayesian model needs to be extended to allow specification of priors on principal stress magnitudes and orientations rather than on stress tensor components only.

These challenges deserve future investigation in order to make full use of the valuable additional sources of stress information available in practice.

6. Summary and conclusions

This paper addresses the crucial problem of how local mean stress estimation can be improved by borrowing information from stress data measured from nearby locations, a generally available and important source that provides additional stress information. Hence, we presented a novel Bayesian hierarchical model that probabilistically quantifies uncertainty in local mean stress estimation and allows for logical borrowing of information across multiple stress data groups from nearby locations. Using both real and simulated stress data, we demonstrated that the proposed hierarchical model can improve local mean stress estimation simultaneously for each location in terms of

uncertainty reduction. We highlighted that the hierarchical model is a generalization of the conventional no pooling and complete pooling models that both rely on overly strict assumptions, and hence should be preferred for local mean stress estimation when stress data from multiple nearby locations are available.

Declaration of competing interest

The authors declare that they have no known competing financial interests or personal relationships that could have appeared to influence the work reported in this paper.

Appendix A

See [Table A.1](#)

Appendix B. Stan codes of the Bayesian hierarchical MVN model

```

data {
  int<lower=1> N;           // number of observations
  int<lower=1> K;           // dimension of observations
  vector[K] y[N];         // observations
  int<lower=1> Ngrp;       // number of groups
  int<lower=1, upper=Ngrp> grp_id[N]; // group id
}

parameters {
  vector[K] mu_tilde[Ngrp];
  corr_matrix[K] Omega;
  vector<lower=0>[K] sigma;
  vector[K] mu0;
  corr_matrix[K] Omega0;
  vector<lower=0>[K] sigma0;
}

transformed parameters {
  vector[K] mu[Ngrp];
  cov_matrix[K] Sigma;
  cov_matrix[K] Sigma0;
  cholesky_factor_cov[K] L0;
  Sigma = quad_form_diag(Omega, sigma);
  Sigma0 = quad_form_diag(Omega0, sigma0);
  L0 = cholesky_decompose(Sigma0);
  for (ngrp in 1: Ngrp) mu[ngrp] = mu0 + L0 * mu_tilde[ngrp];
}

model {
  // hyperpriors
  vector[K] mu1 = [10, 0, 0, 10, 0, 10]';
  matrix[K, K] Sigma1 = diag_matrix([25^2, 7.5^2, 7.5^2, 25^2, 7.5^2, 25^2]');
  mu0 ~ multi_normal(mu1, Sigma1);
  Omega0 ~ lkj_corr(5);
  sigma0 ~ normal(0, 5);

  // priors
  for (ngrp in 1: Ngrp)
    mu_tilde[ngrp] ~ std_normal();
  Omega ~ lkj_corr(5);
  sigma ~ normal(0, 5);

  // likelihood
  for (n in 1: N)
    y[n] ~ multi_normal(mu[grp_id[n]], Sigma);
}

```

References

- Zoback MD. *Reservoir Geomechanics*. Cambridge, UK: Cambridge University Press; 2010.
- Amadei B, Stephansson O. *Rock Stress and its Measurement*. Dordrecht: Springer Netherlands; 1997.
- Zang A, Stephansson O. *Stress Field of the Earth's Crust*. Dordrecht: Springer; 2010:324.
- Hudson JA, Harrison JP. *Engineering Rock Mechanics: An Introduction to the Principles*. Oxford, UK: Pergamon; 1997.
- Mortimer L, Aydin A, Simmons C, Love A. Is in situ stress important to ground-water flow in shallow fractured rock aquifers? *J Hydrol*. 2011;399(3–4):185–200. <http://dx.doi.org/10.1016/j.jhydrol.2010.12.034>.
- Stein RS. The role of stress transfer in earthquake occurrence. *Nature*. 1999;402(6762):605–609. <http://dx.doi.org/10.1038/45144>.
- Ask D. *Analysis of Overcoring Stress Data at the Äspö HRL, sweden - Analysis of Overcoring Rock Stress Measurements Performed Using the CSIRO HI*. Tech. Rep.; Stockholm, Sweden: Swedish Nuclear Fuel and Waste Management Co; 2003.
- Martin CD, Kaiser PK, Christiansson R. Stress, instability and design of underground excavations. *Int J Rock Mech Min Sci*. 2003;40(7–8):1027–1047. [http://dx.doi.org/10.1016/S1365-1609\(03\)00110-2](http://dx.doi.org/10.1016/S1365-1609(03)00110-2).
- Martin CD, Christiansson R. Overcoring in highly stressed granite—the influence of microcracking. *Int J Rock Mech Min Sci Geomech Abstr*. 1991;28(1):53–70. [http://dx.doi.org/10.1016/0148-9062\(91\)93233-V](http://dx.doi.org/10.1016/0148-9062(91)93233-V).
- Pine RJ, Tunbridge LW, Kwakwa K. In-situ stress measurement in the carmenellis granite—I. Overcoring tests at south crofty mine at a depth of 790 m. *Int J Rock Mech Min Sci Geomech Abstr*. 1983;20(2):51–62. [http://dx.doi.org/10.1016/0148-9062\(83\)90327-3](http://dx.doi.org/10.1016/0148-9062(83)90327-3).
- Hakami E, Hakami H, Cosgrove J. *Strategy for a Rock Mechanics Site Descriptive Model - Development and Testing of an Approach to Modelling the State of Stress*. Tech. Rep.; Stockholm, Sweden: Swedish Nuclear Fuel and Waste Management Co; 2002.
- Dzik E, Walker J, Martin C. *A Computer Program (COSTUM) to Calculate Confidence Intervals for in Situ Stress Measurements*. Tech. rep.; Pinawa, Canada: Atomic Energy of Canada Ltd.; 1989.
- Walker JR, Martin CD, Dzik EJ. Confidence intervals for in situ stress measurements. *Int J Rock Mech Min Sci Geomech Abstr*. 1990;27(2):139–141. [http://dx.doi.org/10.1016/0148-9062\(90\)94864-P](http://dx.doi.org/10.1016/0148-9062(90)94864-P).
- Gao K, Harrison JP. Examination of mean stress calculation approaches in rock mechanics. *Rock Mech Rock Eng*. 2019;52(1):83–95. <http://dx.doi.org/10.1007/s00603-018-1568-0>.
- Feng Y, Bozorgzadeh N, Harrison JP. Investigating the effect of sample size on uncertainty in stress estimations. In: *Proceedings of the 52th U.S. Rock Mechanics/Geomechanics Symposium*. Seattle, USA: American Rock Mechanics Association; 2018.
- Feng Y, Harrison JP, Bozorgzadeh N. Uncertainty in in situ stress estimations: a statistical simulation to study the effect of numbers of stress measurements. *Rock Mech Rock Eng*. 2019;52(12):5071–5084. <http://dx.doi.org/10.1007/s00603-019-01891-9>.
- Lei Q, Gao K. A numerical study of stress variability in heterogeneous fractured rocks. *Int J Rock Mech Min Sci*. 2019;113:121–133. <http://dx.doi.org/10.1016/j.ijrmm.2018.12.001>.
- Lei Q, Gao K. Correlation between fracture network properties and stress variability in geological media. *Geophys Res Lett*. 2018;45(9):3994–4006. <http://dx.doi.org/10.1002/2018GL077548>.
- Levandowski W, Herrmann RB, Briggs R, Boyd O, Gold R. An updated stress map of the continental United States reveals heterogeneous intraplate stress. *Nat Geosci*. 2018;11(6):433–437. <http://dx.doi.org/10.1038/s41561-018-0120-x>.
- Feng Y, Bozorgzadeh N, Harrison JP. Bayesian analysis for uncertainty quantification of in situ stress data. *Int J Rock Mech Min Sci*. 2020;134:104381. <http://dx.doi.org/10.1016/j.ijrmm.2020.104381>.
- Wiprut D, Zoback M, Hanssen T-H, Peska P. Constraining the full stress tensor from observations of drilling-induced tensile fractures and leak-off tests: application to borehole stability and sand production on the norwegian margin. *Int J Rock Mech Min Sci*. 1997;34(3–4):365.e1–365.e12. [http://dx.doi.org/10.1016/S1365-1609\(97\)00157-3](http://dx.doi.org/10.1016/S1365-1609(97)00157-3).
- Zoback MD, Moos D, Mastin L, Anderson RN. Well bore breakouts and in situ stress. *J Geophys Res Solid Earth*. 1985;90(B7):5523–5530. <http://dx.doi.org/10.1029/JB090iB07p05523>.
- Feng Y. *Development of Bayesian Approaches for Uncertainty Quantification in in Situ Stress Estimation* (Ph.D. thesis). University of Toronto; 2021.
- Gelman A, Carlin JB, Stern HS, Dunson DB, Vehtari A, Rubin DB. *Bayesian Data Analysis*. third ed. Boca Raton, FL: Chapman and Hall/CRC; 2013.
- Gelman A, Hill J. *Data Analysis using Regression and Multilevel/Hierarchical Models*. Cambridge, UK: Cambridge University Press; 2006. <http://dx.doi.org/10.1017/CBO9780511790942>.
- Lunn D, Jackson C, Best N, Thomas A, Spiegelhalter D. *The BUGS Book: A Practical Introduction to Bayesian Analysis*. CRC Press; 2012.
- Carlin BP, Louis TA. *Bayesian Methods for Data Analysis*. third ed. Boca Raton, FL: CRC Press; 2009:520.

28. Kruschke JK. *Doing Bayesian Data Analysis: A Tutorial with R, JAGS, and Stan*. second ed. Academic Press; 2014.
29. Banerjee S, Carlin BP, Gelfand AE. *Hierarchical Modeling and Analysis for Spatial Data*. second ed. Boca Raton: CRC Press; 2015:583.
30. Freidlin B, Korn EL. Borrowing information across subgroups in phase II trials: is it useful? *Clin Cancer Res*. 2013;19(6):1326–1334. <http://dx.doi.org/10.1158/1078-0432.CCR-12-1223>.
31. Spiegelhalter DJ, Abrams KR, Myles JP. *Bayesian Approaches to Clinical Trials and Health-Care Evaluation*. Chichester, UK: John Wiley & Sons, Ltd; 2003. <http://dx.doi.org/10.1002/0470092602>.
32. Bozorgzadeh N, Bathurst RJ. Hierarchical Bayesian approaches to statistical modelling of geotechnical data. *Georisk: Assess Manag Risk Eng Syst Geohazards*. 2020;1–18. <http://dx.doi.org/10.1080/17499518.2020.1864411>.
33. Bozorgzadeh N, Harrison JP, Escobar MD. Hierarchical Bayesian modelling of geotechnical data: application to rock strength. *Géotechnique*. 2019;69(12):1056–1070. <http://dx.doi.org/10.1680/jgeot.17.P.282>.
34. Lu S, Zhang J, Zhou S, Xu A. Reliability prediction of the axial ultimate bearing capacity of piles: a hierarchical Bayesian method. *Adv Mech Eng*. 2018;10(11). <http://dx.doi.org/10.1177/1687814018811054>.
35. Zhang J, Li J, Zhang L, Huang H. Calibrating cross-site variability for reliability-based design of pile foundations. *Comput Geotech*. 2014;62:154–163. <http://dx.doi.org/10.1016/j.compgeo.2014.07.013>.
36. Broccardo M, Mignan A, Wiemer S, Stojadinovic B, Giardini D. Hierarchical Bayesian modeling of fluid-induced seismicity. *Geophys Res Lett*. 2017;44(22):11,357–11,367. <http://dx.doi.org/10.1002/2017GL075251>.
37. Myers SC, Johannesson G, Hanley W. A Bayesian hierarchical method for multiple-event seismic location. *Geophys J Int*. 2007;171(3):1049–1063. <http://dx.doi.org/10.1111/j.1365-246X.2007.03555.x>.
38. Wainwright HM, Chen J, Sassen DS, Hubbard SS. Bayesian hierarchical approach and geophysical data sets for estimation of reactive facies over plume scales. *Water Resour Res*. 2014;50(6):4564–4584. <http://dx.doi.org/10.1002/2013WR013842>.
39. CEN. *EN 1997-1 Eurocode 7: Geotechnical Design - Part 1: General Rules*. Brussels, Belgium: CEN (European Committee for Standardisation); 2004.
40. Ching J, Phoon K-K. Transformations and correlations among some clay parameters — the global database. *Can Geotech J*. 2014;51(6):663–685. <http://dx.doi.org/10.1139/cgj-2013-0262>.
41. Hoek E, Diederichs M. Empirical estimation of rock mass modulus. *Int J Rock Mech Min Sci*. 2006;43(2):203–215. <http://dx.doi.org/10.1016/j.ijrmms.2005.06.005>.
42. Kim E, Hunt R. A public website of rock mechanics database from earth mechanics institute (EMI) at colorado school of mines (CSM). *Rock Mech Rock Eng*. 2017;50(12):3245–3252. <http://dx.doi.org/10.1007/s00603-017-1292-1>.
43. D'Ignazio M, Phoon K-K, Tan SA, Lämsivaara TT. Correlations for undrained shear strength of finnish soft clays. *Can Geotech J*. 2016;53(10):1628–1645. <http://dx.doi.org/10.1139/cgj-2016-0037>.
44. Gelman A, Pardoe I. Bayesian measures of explained variance and pooling in multilevel (hierarchical) models. *Technometrics*. 2006;48(2):241–251. <http://dx.doi.org/10.1198/004017005000000517>.
45. Barnard J, McCulloch R, Meng X-L. Modeling covariance matrices in terms of standard deviations and correlations, with application to shrinkage. *Statist Sinica*. 2000;10(4):1281–1311.
46. Lewandowski D, Kurowicka D, Joe H. Generating random correlation matrices based on vines and extended onion method. *J Multivariate Anal*. 2009;100(9):1989–2001. <http://dx.doi.org/10.1016/j.jmva.2009.04.008>.
47. McElreath R. *Statistical Rethinking: A Bayesian Course with Example in R and Stan*. second ed. New York, NY: Chapman and Hall/CRC; 2019. <http://dx.doi.org/10.1201/9781315372495>.
48. Stan Development Team. *Stan modeling language users guide and reference manual*. 2021.
49. Obara Y, Sugawara K. Updating the use of the CCBO cell in Japan: overcoring case studies. *Int J Rock Mech Min Sci*. 2003;40:1189–1203. <http://dx.doi.org/10.1016/j.ijrmms.2003.07.007>.
50. Hudson JA, Feng XT. Variability of in situ rock stress. In: *Proceedings of the 5th International Symposium on in-Situ Rock Stress*. Beijing, China: International Society for Rock Mechanics and Rock Engineering; 2010.
51. Harrison JP, Xiang J, Latham JP. Stress heterogeneity in a fractured rock mass modelled with the combined finite-discrete element method. In: *44th U.S. Rock Mechanics Symposium and 5th U.S.-Canada Rock Mechanics Symposium*. Salt Lake City, Utah: American Rock Mechanics Association; 2010.
52. Day-Lewis ADF. *Characterization and Modeling of in Situ Stress Heterogeneity* (Ph.D. thesis). Stanford University; 2008:121.
53. R Core Team. *R: A Language and Environment for Statistical Computing*. Vienna, Austria: R Foundation for Statistical Computing; 2020.
54. Betancourt M. The convergence of Markov chain Monte Carlo methods: from the Metropolis method to Hamiltonian Monte Carlo. *Ann Phys*. 2019;531(3):1700214. <http://dx.doi.org/10.1002/andp.201700214>.
55. Hoffman MD, Gelman A. The no-u-turn sampler: adaptively setting path lengths in Hamiltonian Monte Carlo. *J Mach Learn Res*. 2014;15(1):1593–1623. [arXiv: 1111.4246](http://arxiv.org/abs/1111.4246).
56. Neal RM. MCMC Using Hamiltonian dynamics. In: Brooks S, Gelman A, Jones G, Meng X-L, Neal RM, eds. *Handbook of Markov Chain Monte Carlo*. 2011 [arXiv: 1206.1901v1](http://arxiv.org/abs/1206.1901v1) (Chapter 5).
57. Gao K, Harrison JP. Scalar-valued measures of stress dispersion. *Int J Rock Mech Min Sci*. 2018;106:234–242. <http://dx.doi.org/10.1016/j.ijrmms.2018.04.008>.
58. Pena D, Rodriguez J. Descriptive measures of multivariate scatter and linear dependence. *J Multivariate Anal*. 2003;85(2):361–374. [http://dx.doi.org/10.1016/S0047-259X\(02\)00061-1](http://dx.doi.org/10.1016/S0047-259X(02)00061-1).
59. Feng Y, Harrison JP, Bozorgzadeh N. A Bayesian approach for uncertainty quantification in overcoring stress estimation. *Rock Mech Rock Eng*. 2021;54(2):627–645. <http://dx.doi.org/10.1007/s00603-020-02295-w>.